Peer-reviewed version available at *Materials* **2019**, *12*, 1168; doi:10.3390/ma12071168

Article

Accuracy of eddy-current and radar methods used to reinforcement detection

Łukasz Drobiec [1], Radosław Jasiński [2] and Wojciech Mazur [3*]

Silesian University of Technology, Department of Building Structures; ul. Akademicka 5, 44-100 Gliwice, Poland; radoslaw.jasinski@polsl.pl (R.J.); wojciech.mazur@polsl.pl (W.M.)

* Correspondence: lukasz.drobiec@polsl.pl (Ł.D.); Tel.: +48-32-237-11-27

Abstract: Currently, electromagnetic and radar methods are the most common non-destructive tests for non-destructive rebar location in structures.. Both methods have some advantages, disadvantages and limitations. This article is an attempt to describe possibilities of particular methods with emphasizing their advantages and limitations. The first stage of tests included results from tests conducted on a lintel beam made of autoclaved aerated concrete (AAC) and reinforced with small-diameter rebars and rebars placed close to each other. The second stage consisted in testing nine lightweight concrete specimens, each with three bars having a diameter of 10, 16 and 20 mm at three different space arrangements, to determine the effect of bar diameter and spacing on the measurement accuracy. The reinforcement of lintels and specimens was tested with two different electromagnetic scanners and a ground-penetrating radar (GPR) device. Received results from direct tests were compared with results from non-destructive tests (NDT). NDT tests conducted in such an element were found to perform the correct assessment of the concrete cover, and at the same time to give ambiguous results with reference to shape and number of rebars.

Keywords: NDT Methods, Rebar location, Eddy-current method, GPR method

1.Introduction

Non-destructive testing is becoming more and more common in the construction sector. Tests are performed on existing structures which require reconstruction, extension or reinforcement, and on new structures as a part of works connected with the acceptance stage. Tests are also carried out if some irregularities concerning material strength or the quantity of applied reinforcement, are suspected. In reinforced structures, in contrast to steel and wood structures, rebars – elements providing bearing capacity in zones subjected to tensile strength, are invisible. Consequently, the majority of diagnostic methods applied in practice refer to localisation of reinforcement and measuring diameters of rebars in reinforced structures. Tests are usually conducted on slab and beam elements. However, significant errors regarding the precision of made measurements can be observed.

The geometry of rebars can be determined with the traditional method by performing pits or with non-destructive testing (NDT) [1, 2]. NDT methods are useful especially when tests are to be conducted on a wide surface or many elements. Electromagnetic and radar methods are currently the most often used NDT methods for detecting reinforcement in the structure [2, 3, 4]. Both methods have their advantages and disadvantages. It can be assumed that advantages of the electromagnetic method are: the accuracy of measurements and the possibility for determining the diameter of reinforcement. And its disadvantages include a short range of measurements and some errors triggered by resolution, which are significant when rebars are closely arranged(lap splices, bundles of bars) [5, 6]. The advantage of the radar method is the possibility for localising the reinforcement at great depths; and its disadvantages cover difficulties in measuring diameters measurements and some measurement errors of damp structures [7, 8].

Despite the continuous development, electromagnetic and radar methods still have some limitations. Many reference papers present advantages and possibilities for using electromagnetic

and radar methods. Information about their limitations and measurement accuracies is rarely published. According to the definition [9], the accuracy is a compatibility level between the obtained result of a single measurement and the expected value related to systematic and accidental errors. However, design standards and standards specifying structures reinforced with bars permit some execution deviations. Thus, it seems interesting whether the real accuracy of methods is within standard limits of execution deviations.

This article presents problems encountered during detection and measurements of reinforcement with radar and electromagnetic methods. The aim of this article was to test whether measurement uncertainties could be higher than allowable performance uncertainties. Reinforced lintel beams made of autoclaved aerated concrete (AAC) were tested with three different types of measurement devices. Measurement errors were analysed, and obtained results were compared to deviations accepted by standards. This analysis included adequate estimators of uncertainty.

2. Accuracy and possibilities of non-destructive testing

2.1. Electromagnetic method

The accuracy of electromagnetic tests mainly depends on the location depth, spacing, arrangement of rebars toward the direction of scanning, the type of reinforcement, and the quality of concrete surface [10, 11]. A type of spectral analysis and compensation procedures of systematic measuring errors also affect the accuracy of tests .

The depth of bars location has a significant impact on the accuracy of diameter measurements, and even on the accuracy of bars location. The maximum depth, at which reinforcement can be detected, depends on the diameter of rebars. For typical rebar diameters of 6÷25 mm, depending on the employed device, the biggest depth at which the reinforcement can be detected is 100 ÷ 200 mm. Closer location of rebars to the scanned surface evidently ensures a greater accuracy of the measured and real diameter. The acceptable measurement accuracy (5%) of the reinforcement diameter is obtained when rebars are located at a depth of ca. 60 mm.

A measurement is made with a single-frequency or a multi-frequency method. Tests on reinforced concrete structures often employ multi-frequency signals of sinusoidal type A sinusoidal excitation signal emitted inside the structure, depends on time t. Therefore, the excitation W(t)can be expressed [12, 13] with a harmonic function:

$$W(t) = \sum_{1}^{N} w_i \sin\left(\omega_{wi} t + \varphi_{wi}\right), \tag{1}$$

where:
w_i – the amplitude of i-th wave of sinusoidal input,
ω_i – pulsation of i-th wave of sinusoidal input,
φ_{wi} – phase angle of i-th wave of sinusoidal input.

Assuming that the reinforcement in the tested element causes linear changes of the input function, a signal y(t) received by measuring coil is :

$$y(t) = \sum_{1}^{N} k_{wi} w_i \sin\left(\omega_{yi} t + k_{i\varphi} \varphi_{yi}\right), \tag{2}$$

where:
k_{wi} – the amplitude factor of received i-th sinusoidal wave,
ω_{yi} – pulsation of received i-th sinusoidal wave,
$k_{i\varphi}$ – change factor of the phase angle of received i-th sinusoidal wave,
φ_{yi} – phase angle of received i-th sinusoidal wave.

The assumption of a linear change of the sinusoidal input indicates that the pulsation of the excitation signal and the received signal are equal:

$$\omega_{wi} = \omega_{yi}, \tag{3}$$

On this basis the function y(t)can be expressed as:

$$y(t) = \sum_{1}^{N} k_{wi} w_i \sin\left(\omega_{wi} t + k_{i\varphi} \varphi_{yi}\right). \tag{4}$$

The information about reinforcement geometry is included in coefficients k_{wi} and $k_{\varphi i}$. A signal $y(t)$ is recorded in RAM memory of the probe. Then, the measuring signal is subjected to processing, which usually consists in converting into a digital signal and performing a spectral analysis. Amplitudes of sinusoidal components are the most important parameters in case of reinforcement measurements. A microprocessor of the testing device computes and analyses measured amplitudes of sinusoidal components, which is the base for estimating the diameter and the depth of reinforcement. Signal of transducers is often processed using inverse models based on dynamic neural networks [14].

The paper [11] describes tests to detect plain and ribbed rebars of 12 diameter. Tests were done with four different devices. Variations of the measured thickness of the concrete cover were within 4 mm, and the measured reinforcement diameter differed by not more than one gradation. The paper [15] presents the analysis of measurement errors of the electromagnetic device in slabs having dimensions of 400x400x250 mm , made of high compressive strength concrete (average 71.3 N/mm^2). One rebar was placed in each slab. Rebars of 12, 16, 20, 25 and 32 mm diameter and 50 and 100 mm covers were used (in total 10 of test models). Fig. 1 illustrates the graph of the relative measuring error of the reinforcement diameter as a function of the concrete cover size. The acceptable error (<10%) was obtained for the cover thickness of up to ca. 40 mm. It should be emphasized that although the paper [15] is relatively recent, the used device is not a modern one. As no tests on the models of concrete with lower strength were conducted, it is hard to define the influence of the high compressive strength concrete. In typical reinforced concrete structures (beams, slabs, columns) with standard covers (c ~ 20-45 mm), available in practice electromagnetic devices can be used to perform tests with accuracy of the measurement less than 10%. The gradation of rebar diameters causes difficulties in diameter differentiation.

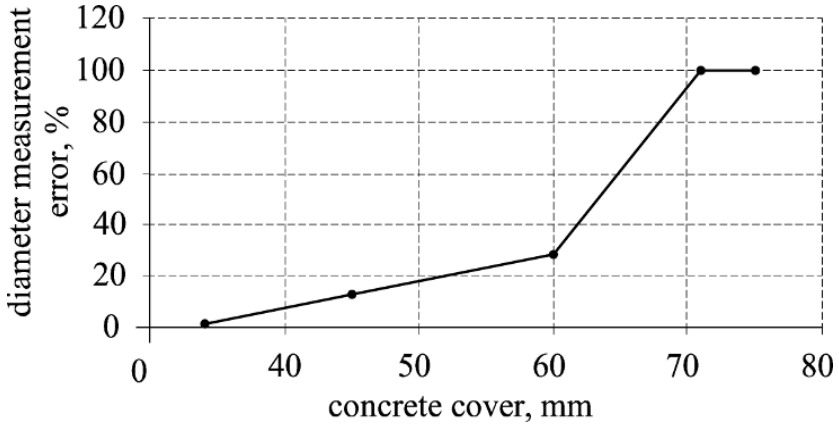

Figure 1. The error of the reinforcement diameter measured with an electromagnetic device, depending on the cover size according to [15]

2.2. Radar method

In the radar method, the measuring range of the structure depth depends on concrete structure, a type of an antenna, and frequencies of the excited impulse [16, 17, 18]. In typical devices, this range

is up to 750 mm. The image contrast obtained from radar tests depends on relative difference between dielectric constant values at the contact area between materials. There are no difficulties in interpreting the obtained image because of considerable differences in constant values for concrete and steel. Tests on reinforcement location conducted with radar method generate radargrams, that is, the record of all reflected signals registered during the passage of a measuring probe on the element surface. The reinforcement image on radargram is a distortion of course contour lines in the shape of hyperbola arms directed down the radargram.

The modern measurement systems perform the automatic analyses of radargrams, convert radargrams taken close to each other in one image, and visualize reinforcement in the construction in a legible way for users. The additional software can be used to take a spatial image of the structure with the reinforcement. The radar devices do not give direct information about reinforcement diameters. Maybe measurements in a 3D model can be a solution for this problem. However, some published articles present some mathematical correlations between the shape of a hyperbola shown on the radargram and the reinforcement diameter. Devices with the option of determining the reinforcement diameter are likely to appear soon on the market. However, the accuracy of the measurement method might be still a problem. Currently, the accuracy of the cover measurements with radar method performed with the best devices is defined as ± 5 – 10 mm.

The papers [19, 20, 21, 22, 23, 24, 25] describe that the shape of hyperbola illustrating the reinforcement on the radargram depends on the wave propagation velocity υ and passage time $t_0$of measuring probe above the tested reinforcement. The time of the measuring probe passage is the time passing from the moment when the device records the reinforcement for the first time till the moment when it stops to record it. The velocity of the wave propagation affects the hyperbola curve, whereas the time of the probe passage affects the range of its arms. Knowing parameter values a and b of the hyperbola b (Fig. 2), their relation with the reinforcement diameter ϕ, wave propagation velocity υ and time of probe passage t_0, on the tested reinforcement can be expressed as following:

$$a = t_0 + \frac{\phi}{\upsilon}, \tag{5}$$

$$b = \frac{\upsilon}{2}\left(t_0 + \frac{\phi}{\upsilon}\right). \tag{6}$$

The wave propagation velocity υ and passage time $t_0$of the measuring probe are recorded by a measuring device; and parameters a, b can be read from the radargram. Therefore, there are no obstacles to determine the reinforcement diameter ϕ from equations (5 and 6). The paper [26] confirms the possible usage of this method for defining the reinforcement as under laboratory conditions obtained the measuring error of diameters of steel pipes and cables was in the order of 1.7÷5.3%.

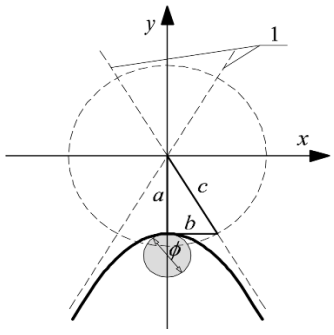

Figure 2. Assumptions to derive equations (5 and 6), 1 - hyperbola asymptotes

The paper [27] proposes another way of defining the diameter. It was assumed that the impulse distribution angle from the transmitting antenna was 90° (Fig. 3). Such an assumption was useful for determining the rebar diameter without taking into account the wave propagation velocity υ and

Preprints (www.preprints.org) | NOT PEER-REVIEWED | Posted: 5 March 2019 doi:10.20944/preprints201901.0014.v2

Peer-reviewed version available at Materials 2019, 12, 1168; doi:10.3390/ma12071168

passage time $t_0$of the measuring probe above the tested reinforcement. Reinforcement diameter ϕ can be determined according to:

$$\phi = 2\sqrt{2}L - 2X - 2Y, \tag{7}$$

where:
L, X, Y – geometric data according to Fig. 3.

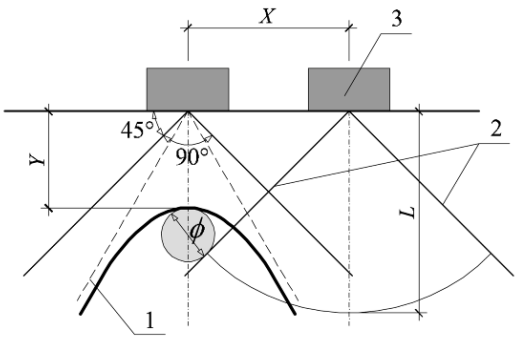

Figure 3. Assumptions to derive the equation (7), 1 - hyperbola asymptotes, 2 – the angle of impulse distribution from the antenna, 3 – a measuring probe

2.3. Combination of electromagnetic and radar methods

The papers [28, 29] suggest connecting advantages of electromagnetic and radar methods. Tests were conducted on specimens placed in a pen and in concrete. Rebar diameters were tested in rebar laboratories. The electromagnetic method was found not to give correct test results because the reinforcement was placed too close. On the basis of conducted tests, the empirical equations were developed to estimate the diameter of contact rebars in the rebar laboratory. The accuracy of determined diameters was obtained at the level of 2.35%. Empirical equations were observed to have some application limitations regarding the tested reinforcement and concrete.

To sum up, the advantage of devices working according to the electromagnetic method was their high accuracy at small depths of measurements. A small range of diameter measurements, limited to about 6 cm, is their disadvantage Radar devices have much bigger range (even up to 75 cm).However devices available on market do not offer the possibility of diameter measurements. In the world, some methods for diameter determining on the basis of radargram measurements obtained from the radar tests are being developed. Radar devices with the option of diameter measuring are likely to appear soon on the market.

3. Tested specimens

3.1. AAC precast lintels

To verify the accuracy of NDT methods, some tests were performed on widely used lintels made of AAC with the width of b = 180 mm, height h = 240 mm and the total length of L = 2000 mm. The strength of AAC elements was f = 4 N/mm^2. Detailed results from material tests on lintelsare presented in the papers [30, 31, 32]. The lintel reinforcement was made of steel with yield strength of 500 N/mm^2 (B class, according to EN 1992-1-1:2008). Longitudinal rebars had a diameter of 8 mm (three rebars down and two rebars up). Longitudinal reinforcement in the form of open stirrups made of rebars having a diameter of 4.5 mm. Stirrups were placed along the whole element at a constant spacing of 150 mm (Fig. 4). The longitudinal reinforcement and stirrups were welded and covered with corrosion-resistant protective coating made of resin.

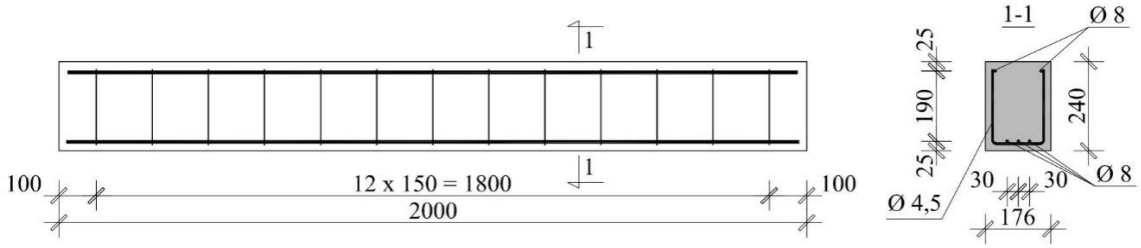

Figure 4. Dimensions and reinforcement of the tested lintel

Two beams were selected for tests. To ensure precise location of the reinforcement, both ends of tested beams were broken down and the reinforcement was measured– Fig. 5. Tiny openings (diameter of 2 mm) were made in 11 places on lateral surfaces and at the bottom 8 points (between the stirrups)(at points of non-destructive testing)to measure the real reinforcement cover – c_{obs} with accuracy of $\Delta c_{obs} = \pm 0{,}1$ mm. Because the location of both beams was the same, tests were conducted only on one of them.

Figure 5. The view of tested elements with the reinforcement broken down at its ends

3.2. Lightweight concrete specimens

The impact of bar diameter and spacing on the measurement accuracy was tested on nine models (Fig. 6) prepared from lightweight concrete with density of 0.9 kN/m^3 and strength of 10.2 N/mm^2 after 7 days and of 18.1 N/mm^2 after 28 days. Each model had three bars arranged in such a way to ensure the distance between bars equal 20, 30 and 40 mm (dimension "a" in Fig. 6). The diameter of used bars was ø = 10; 16 and 20 mm. Dimensions of models in a plain view were 240x440 mm 40, 60 and 80 mm thick. Different thickness was to ensure the correct (two-sided) cover of rebars with concrete assuming that rebar distance from the tested surface was 20 mm. And wooden washers were applied for that purpose. Reinforcement was laid using wooden spacers of relevant thickness (Fig. 7a), and then stabilized in washers with screws (Fig. 7b). Concrete was laid, mechanically compacted and properly cured. Fig. 8 shows models before and after concreting. Labelling of specimens contained a letter S, diameter *d* and space between bars *a*. For example, S-15-30 identifies a specimen reinforced with three bars having a diameter of 16 mm and space between rebars equal to 30 mm.

Preprints (www.preprints.org) | NOT PEER-REVIEWED | Posted: 5 March 2019 doi:10.20944/preprints201901.0014.v2

Peer-reviewed version available at Materials 2019, 12, 1168; doi:10.3390/ma12071168

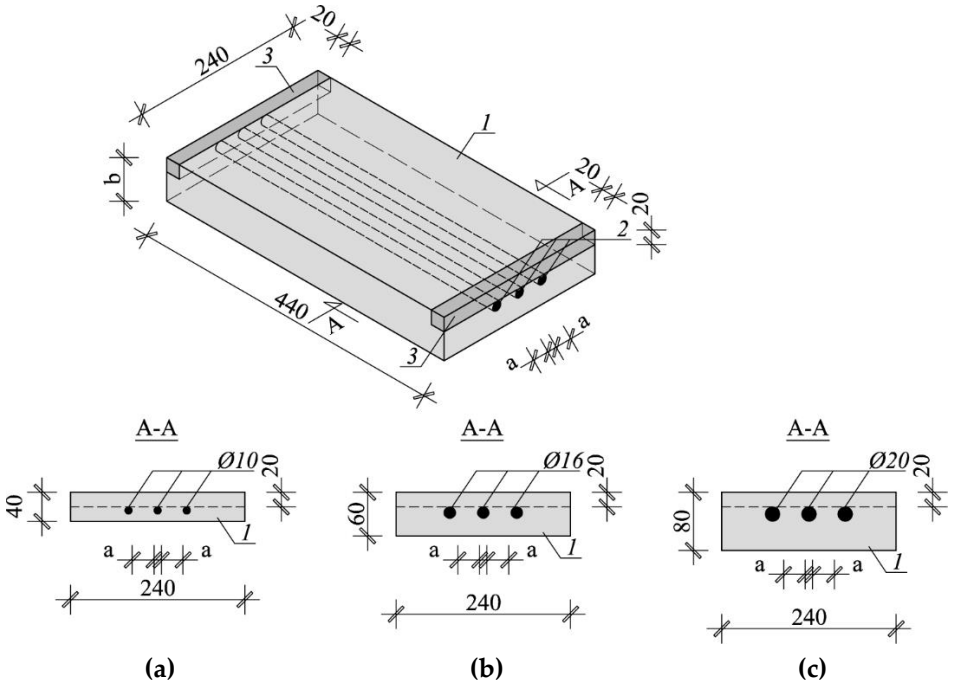

Figure 6. Lightweight concrete specimens: (**a**) specimen reinforced with bars of 10 mm diameter, **(b)** specimen reinforced with bars of 16 mm diameter, **(c)** specimen reinforced with bars of 20 mm diameter, 1 – lightweight concrete, 2 – rebars, 3 – wooden washer

Figure 7. Reinforcement stabilization in formwork: (**a**) distance resulting from wooden spacers, (**b**) fastening rebars to wooden washers with screws

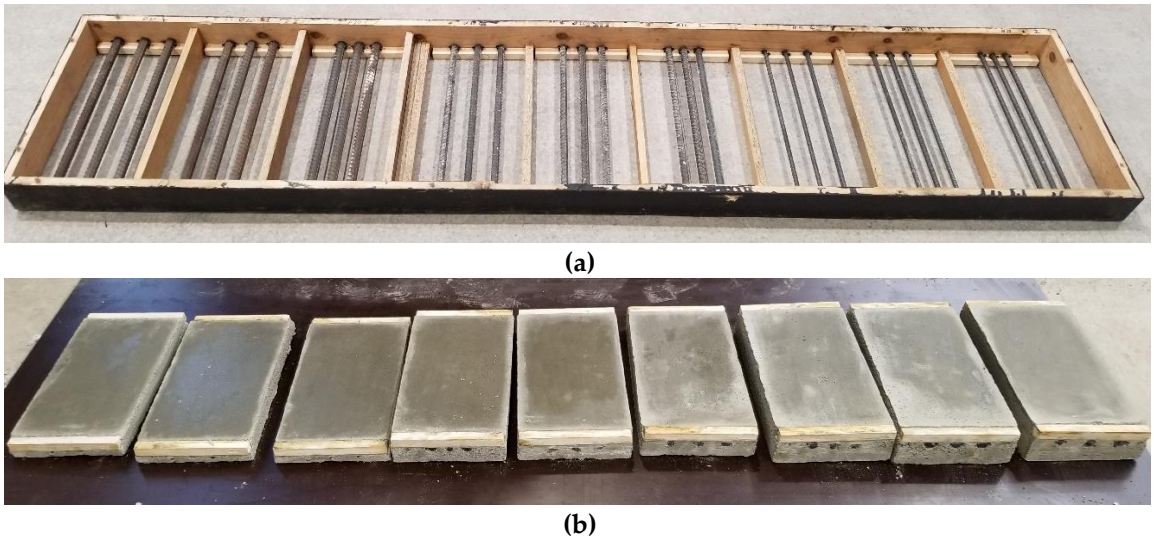

Figure 8. Specimen reinforcing in formwork (**a**) and specimens after concreting (**b**)

4. Applied research equipment

Tests were conducted using two electromagnetic scanners: PS 200 (manufacturer Hilti Corp., Schaan, Lichtenstein) Profometer 630 AI (manufacturer Proceq AG, Schwerzenbach, Switzerland) and one GPR device –GPR Live (manufacturer Proceq AG, Schwerzenbach, Switzerland). The devices are shown in fig. 9. A scanning transducer of the electromagnetic device 1 was equipped with one circumferential transmitting coil and seven pairs of receiving coils. Receiving coils induce current with microammeters, and the received signal is then processed and analysed. The electromagnetic device no. 2 is similar in principle. The radar equipment 3 was equipped with antennas to perform tests, using a signal with a variable frequency within a range of 0.2-4.0 GHz. During tests, frequency was changed progressively in an automatic way, and max. acquisition time 20 ns.

The measuring accuracy of each device was the same, $\Delta c_{obs} = \pm 1.0$ mm(according to information provided by device manufacturers).

(a) **(b)** **(c)**

Figure 9. The view of devices used in tests, (**a**) electromagnetic device (1), (**b**) electromagnetic device (2), (**c**) radar device (3)

5. Miejsca badań

5.1. AAC precast lintels

Tests were performed with each device by scanning the same points of the beams on the lateral surface and from the bottom. Stirrup rebars were detected on the lateral surface, whereas the main reinforcement was tested from the bottom. Tests were conducted with line and area scans

Fig. 10a illustrates places of area scans for testing stirrups, and Fig. 10b presents area scans for testing the main reinforcement. The location of linear scan and the point of measuring stirrups are shown in Fig. 10c, whereas the location of linear scan for the main reinforcement is shown in Fig. 10d.

Preprints (www.preprints.org) | NOT PEER-REVIEWED | Posted: 5 March 2019 doi:10.20944/preprints201901.0014.v2

Peer-reviewed version available at Materials 2019, 12, 1168; doi:10.3390/ma12071168

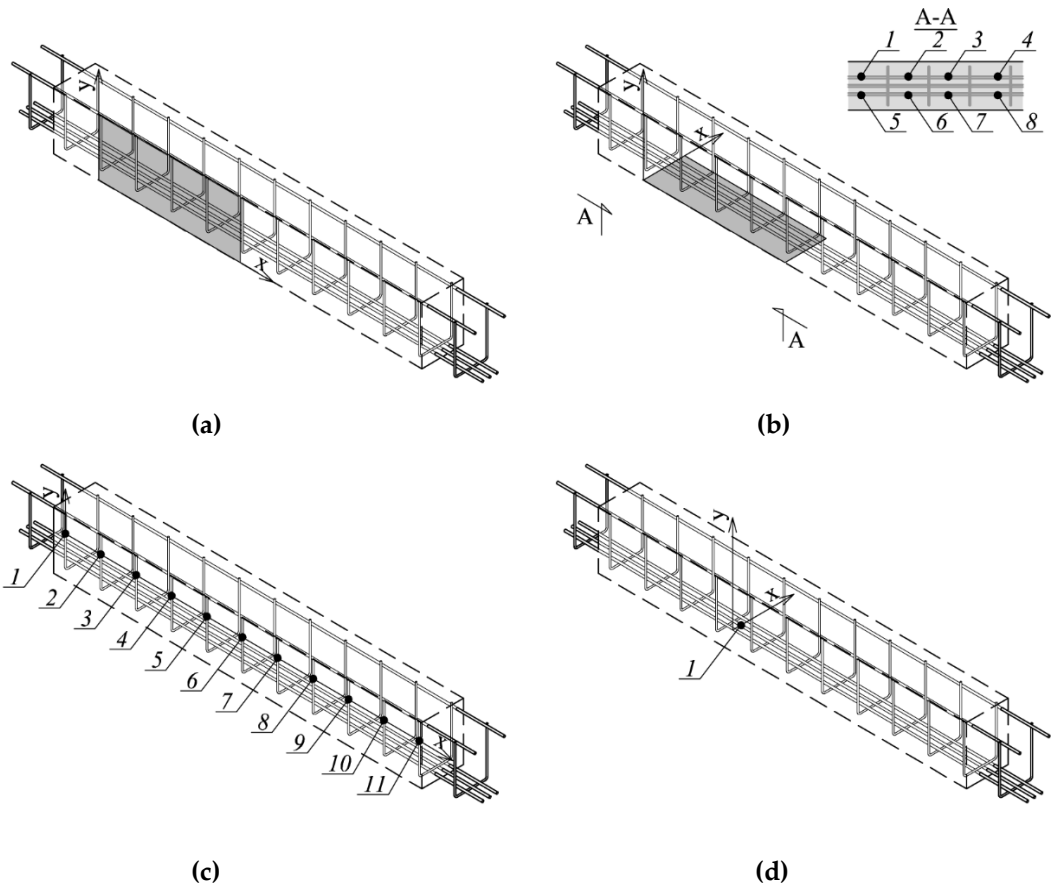

Figure 10. Places of lintel tests: (**a**) Stirrup tests – area scan (measurement in the grey-coloured field), (**b**) main reinforcement test – area scan (measurement in the grey-coloured field, measurement at points 1-8), (**c**) Stirrup tests – line scan (measurement at points 1-11), (**d**) main reinforcement test – line scan (measurement at point 1)

5.2. Lightweight concrete specimens

Lightweight concrete specimens were tested using the electromagnetic equipment (1) over the area of 150x300 mm illustrated in Fig. 11a. The electromagnetic equipment (2) was used to perform linear scans at the mid-length of the specimen (Fig. 11b), while area scans were made with the radar equipment over the area of 200x300 mm shown in Fig. 11c. Scans were always taken in a place where the cover thickness was 20 mm. Fig. 12 shows types of used equipment

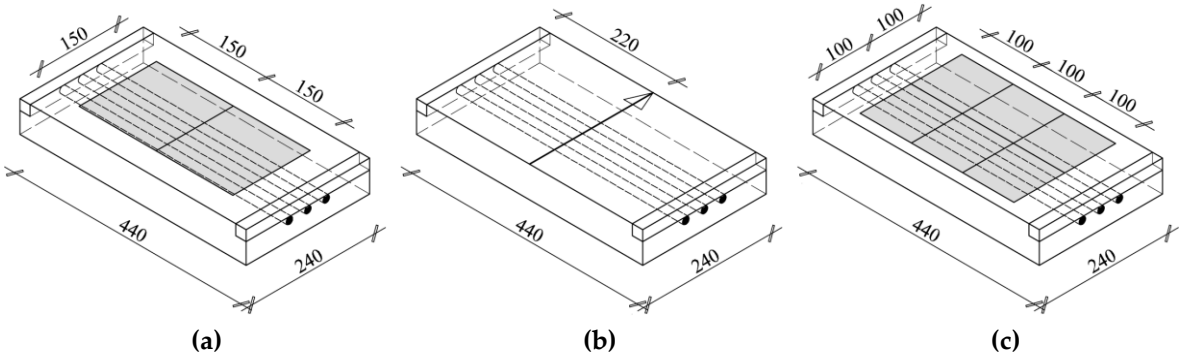

Figure 11. Location of tests performed with: (**a**) electromagnetic device (1), (**b**) electromagnetic device (2), (**c**) radar device (3)

Preprints (www.preprints.org) | NOT PEER-REVIEWED | Posted: 5 March 2019 doi:10.20944/preprints201901.0014.v2

Peer-reviewed version available at Materials 2019, 12, 1168; doi:10.3390/ma12071168

(a) (b) (c)

Figure 12. Testing specimens with: (**a**) electromagnetic device (1), (**b**) electromagnetic device (2), (**c**) radar device (3)

6. Test results

6.1. AAC precast lintels (AAC)

6.1.1. Stirrups tests

Stirrups were tested at the beam side as line and area scans. Line scans can be only used to determine the reinforcement location (spacing and concrete cover). Fig. 13 illustrates the comparison of exemplary results from line scans taken with electromagnetic devices and the radar device (radargram). A great conformity between test results and real measurements of bar location was found. Fig. 14 presents examples of area scans taken with the electromagnetic device 1 and the radar device 3. Area scans taken with two methods, showed very clearly both stirrup reinforcement and longitudinal reinforcement.

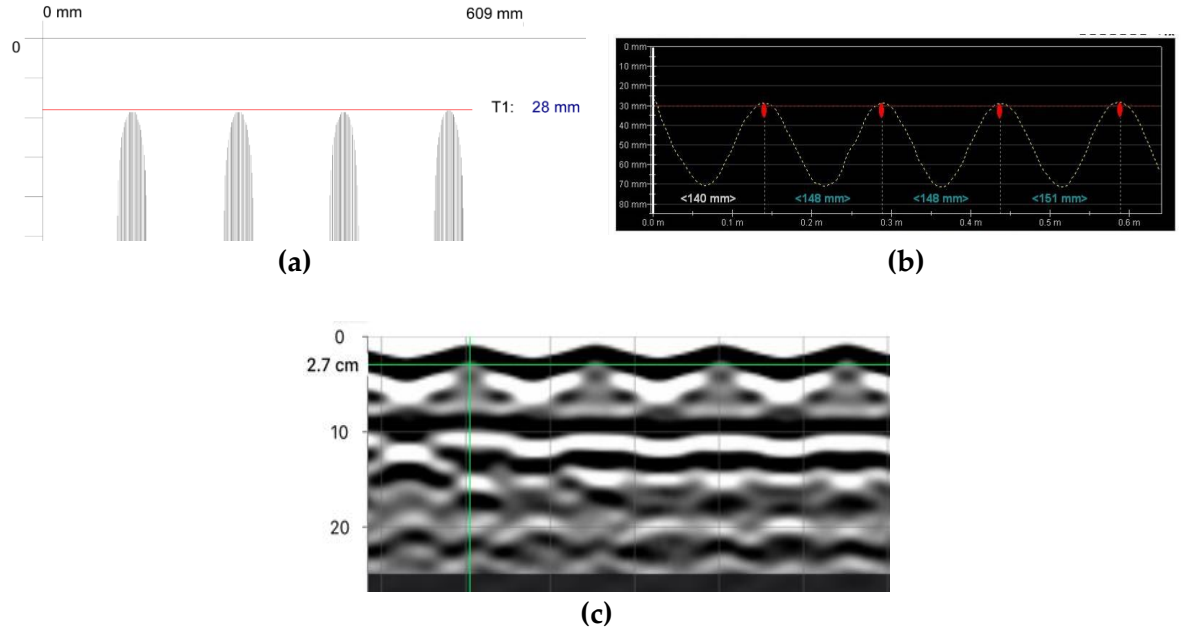

(a) (b) (c)

Figure 13. Line scans (measurement at points shown in Fig. 10c) with devices: (**a**) electromagnetic 1, average cover of visible results– 27.8 mm, (**b**) electromagnetic 2, average cover – 28.6 mm, (**c**) radar 3, average cover 27 mm

Preprints (www.preprints.org) | NOT PEER-REVIEWED | Posted: 5 March 2019 doi:10.20944/preprints201901.0014.v2

Peer-reviewed version available at Materials 2019, 12, 1168; doi:10.3390/ma12071168

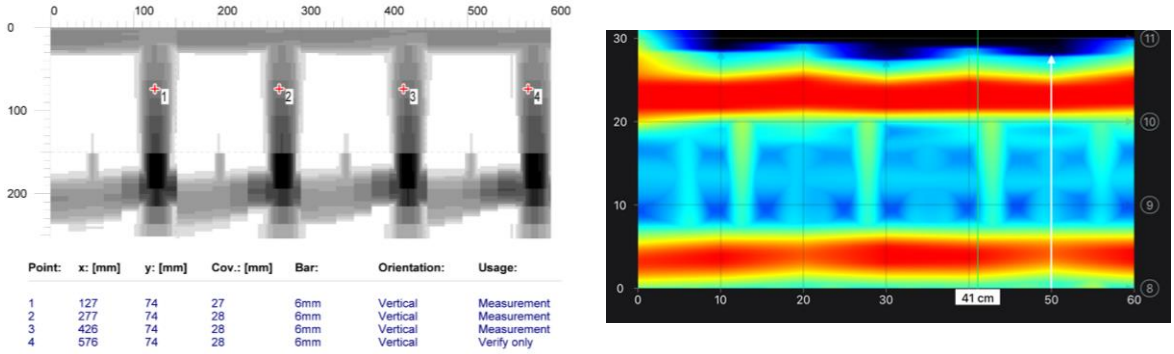

(a) **(b)**

Figure 14. Area scans with electromagnetic devices (measurement on the area shown in Fig. 10a), (**a**) electromagnetic 1, average cover of visible results– 27.8 mm, (**b**) radar 3,– 27 mm

6.1.2. Tests on longitudinal rebars

The aim of testing the main reinforcement tests, made from the beam bottom, was to determine the size of the cover, the number and diameters of rebars in the main reinforcement (diameters were determined only in case of electromagnetic scans). Fig. 10shows the comparison ofresults from electromagnetic tests. The area scan (Fig. 15a), was taken with the electromagnetic device 1 and line scan (fig 15b) was taken with the electromagnetic device 2. Both devices did not detect the correct number of rebars. The device 1 detected two rebars instead of three, but it measured the diameter quite correctly. However, the device 2 detected only one rebar and gave the diameter equal to 18 mm. Results from tests performed with the GPR device are shown in Fig. 16. Area and line scans were taken. The line scan is presented as the radargram (Fig. 16a), and the area scan as a map (Fig. 16b). Only one longitudinal rebar was detected during both tests using the radar method.

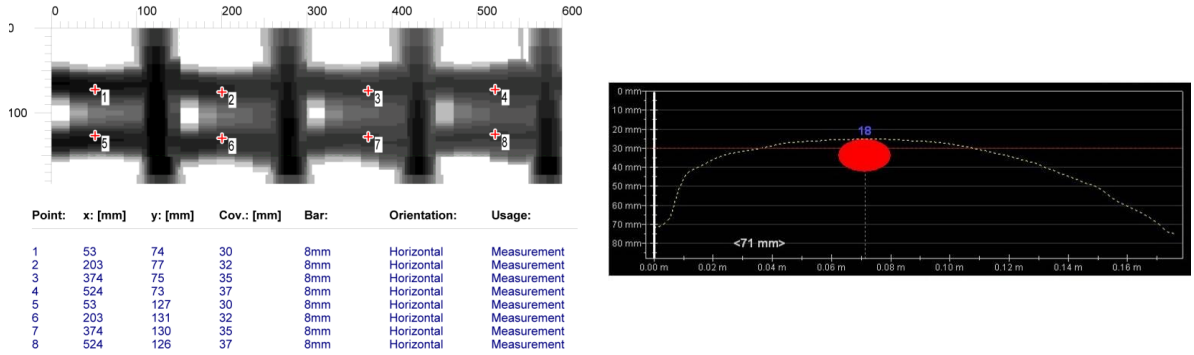

(a) **(b)**

Figure 15. Scans taken with electromagnetic devices, (**a**) device 1, two rebars detected, average cover of visible results – 33.6 mm, diameter 6-8 mm (measurement on the area shown in Fig. 10b), (**b**) device 2, one rebar detected, average cover of visible results – 28 mm, diameter 18 mm (measurement at the point shown in Fig. 10d)

To sum it up, test results for the longitudinal reinforcement, in which rebars were closer to each other (an axial spacing of rebars was 30 mm – Fig. 4) were poorer than in case of tests performed on stirrup reinforcement as described in point 6.1.1. None of devices used during various methods of testing, correctly detected the number of longitudinal rebars. The most satisfactory result was observed for tests performed with the electromagnetic instrument 1.

Preprints (www.preprints.org) | NOT PEER-REVIEWED | Posted: 5 March 2019 doi:10.20944/preprints201901.0014.v2

Peer-reviewed version available at Materials 2019, 12, 1168; doi:10.3390/ma12071168

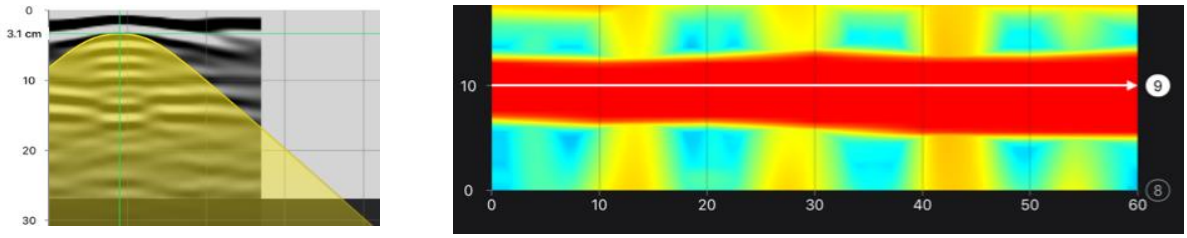

(a) (b)

Figure 16. Scans taken with the radar (3), one rebar detected, (**a**) line scan (radargram- measurement at the point shown in Fig. 10d), (**b**) area scan (measurement on the area shown in Fig. 10b)

6.2. Lightweight concrete specimens

Tests on lintel beams indicated significant errors in measuring the quantity of reinforcement and the number of rebars in the main reinforcement. Thus, additional tests were performed on lightweight models prepared for this purpose. The aim of those tests was to capture the relationship between rebar diameters and spacing and the accuracy of measurements. Fig. 17 shows results from tests conducted with the electromagnetic equipment (1). They contain the measured number and diameter $ø_{obs}$ of rebars and average cover c_{obs}. .

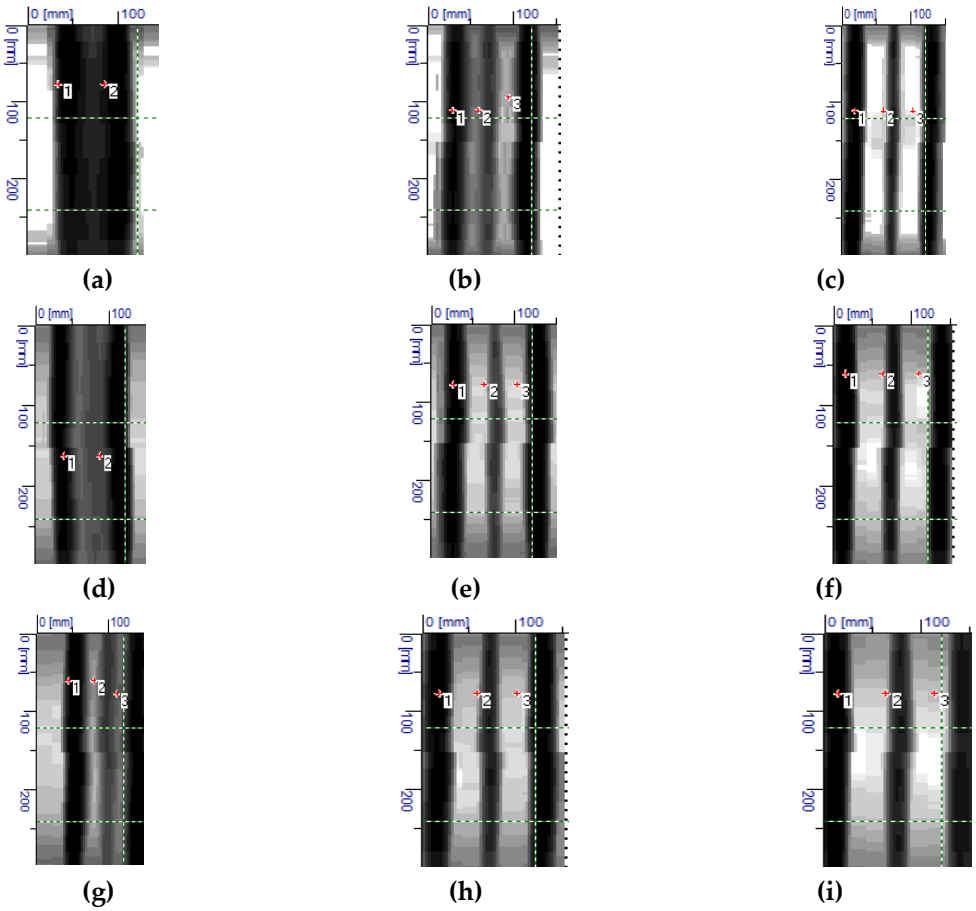

(a) (b) (c)

(d) (e) (f)

(g) (h) (i)

Figure 17. Results from tests conducted with the electromagnetic device (1): (**a**) S-10-20 (result: 2 bars, $ø_{obs}$ = 8 mm, c_{obs} = 25 mm), (**b**) S-10-30 (3 bars, $ø_{obs}$ = 8 mm, c_{obs} = 20 mm), (**c**) S-10-40 (3 bars, $ø_{obs}$ = 10 mm, c_{obs} = 21 mm), (**d**) S-16-20 (2 bars, $ø_{obs}$ = 30 mm, c_{obs} = 25 mm), (**e**) S-16-30 (3 bars, $ø_{obs}$ = 16 mm, c_{obs} = 18 mm), (**f**) S-16-40 (3 bars, $ø_{obs}$ = 20 mm, c_{obs} = 20 mm), (**g**) S-20-20 (3 bars, $ø_{obs}$ = 20 mm, c_{obs} = 25 mm), (**h**) S-20-30 (3 bars, $ø_{obs}$ = 20 mm, c_{obs} = 18 mm), (i) S-20-40 (3 bars, $ø_{obs}$ = 20 mm, c_{obs} = 22 mm)

Preprints (www.preprints.org) | NOT PEER-REVIEWED | Posted: 5 March 2019 doi:10.20944/preprints201901.0014.v2

Peer-reviewed version available at Materials 2019, 12, 1168; doi:10.3390/ma12071168

As in case of testing the lintel beam, tests failed to detect the correct number of rebars spaced at a_{nom} = 20 mm for specimens reinforced with bars having a diameter $ø_{nom}$ = 10 mm. In case of the specimen at the similar space, but reinforced with bars $ø_{nom}$ = 16 mm, three bars could be spotted, but only two of them were detected with the equipment which also provided the excessive diameter of 30 mm. The equipment identified 3 rebars of 20 mm diameter, at the minimum spacing, but indicated the diameter twice smaller (10 mm). At larger spacing a_{nom} = 30 and 40 mm, the electromagnetic equipment (1) detected the correct number of rebar diameter, but some inaccuracies were found while measuring covers.

Fig. 18 shows results from tests conducted with the electromagnetic equipment (2). As above, results include the number of rebars and their measured diameters d and the average size of tested concrete cover c. For the smallest diameter and spacing, the equipment detected only one bar just as in case of tests on precast beam. The equipment found 3 rebars in specimens reinforced with bars of 16 and 20 mm diameter spaced at more than 20 mm. Some deviations were observed in measured diameters and covers. Contrary to the electromagnetic equipment (1), the equipment (2) provided more accurate diameters with less precisely measured thickness of concrete cover. Differences in cover measurements were even up to 5 mm

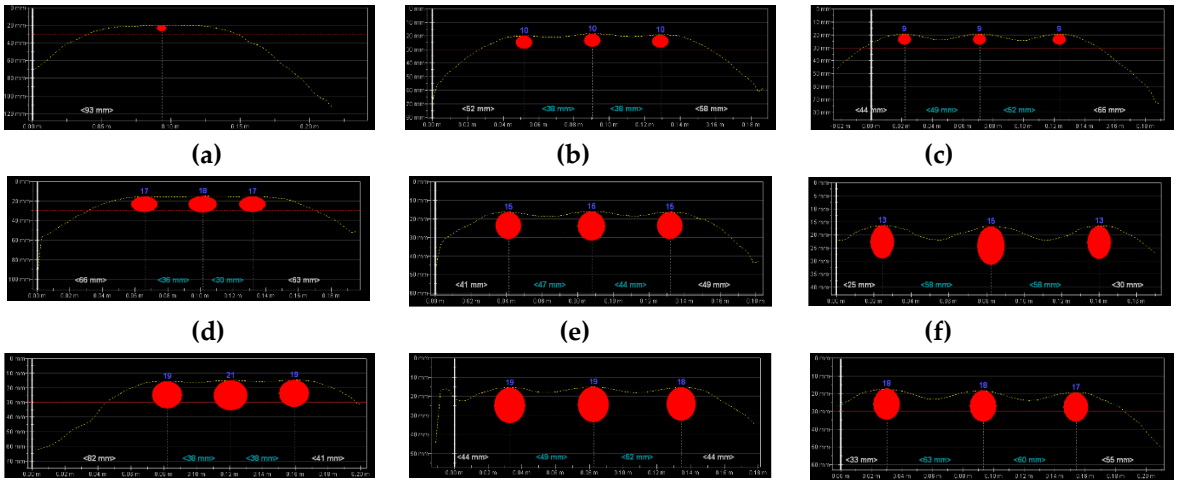

Figure 18. Results from tests performed with the electromagnetic device (2): (**a**) S-10-20 (result: 1 bar, $ø_{obs}$ = 8 mm, c_{obs} = 20 mm), (**b**) S-10-30 (3 bars, $ø_{obs}$ = 10 mm, c_{obs} = 19.3, mm), (**c**) S-10-40 (3 bars, $ø_{obs}$ = 9 mm, c_{obs} = 19.3 mm), (**d**) S-16-20 (3 bars, $ø_{obs}$ = 17 mm, c_{obs} = 15.5, mm), (**e**) S-16-30 (3 bars, $ø_{obs}$ = 15 mm, c_{obs} = 16.4, mm), (**f**) S-16-40 (3 bars, $ø_{obs}$ = 14 mm, c_{obs} = 16.5, mm), (**g**) S-20-20 (3 bars, $ø_{obs}$ = 19 mm, c_{obs} = 15 mm), (**h**) S-20-30 (3 bars, $ø_{obs}$ = 19 mm, c_{obs} = 15.4 mm), (i) S-20-40 (3 bars, $ø_{obs}$ = 18 mm, c_{obs} = 18.3 mm)

Results include the number and average size of tested concrete cover c_{obs}. The correct number of rebars was detected in all tested specimens. The measured value of covers also showed high compliance with the true value (20 mm) No possibility of taking direct measurements of diameter was a drawback of the radar equipment. Therefore, there are no rebar diameters in Fig. 18.

Preprints (www.preprints.org) | NOT PEER-REVIEWED | Posted: 5 March 2019 doi:10.20944/preprints201901.0014.v2

Peer-reviewed version available at Materials 2019, 12, 1168; doi:10.3390/ma12071168

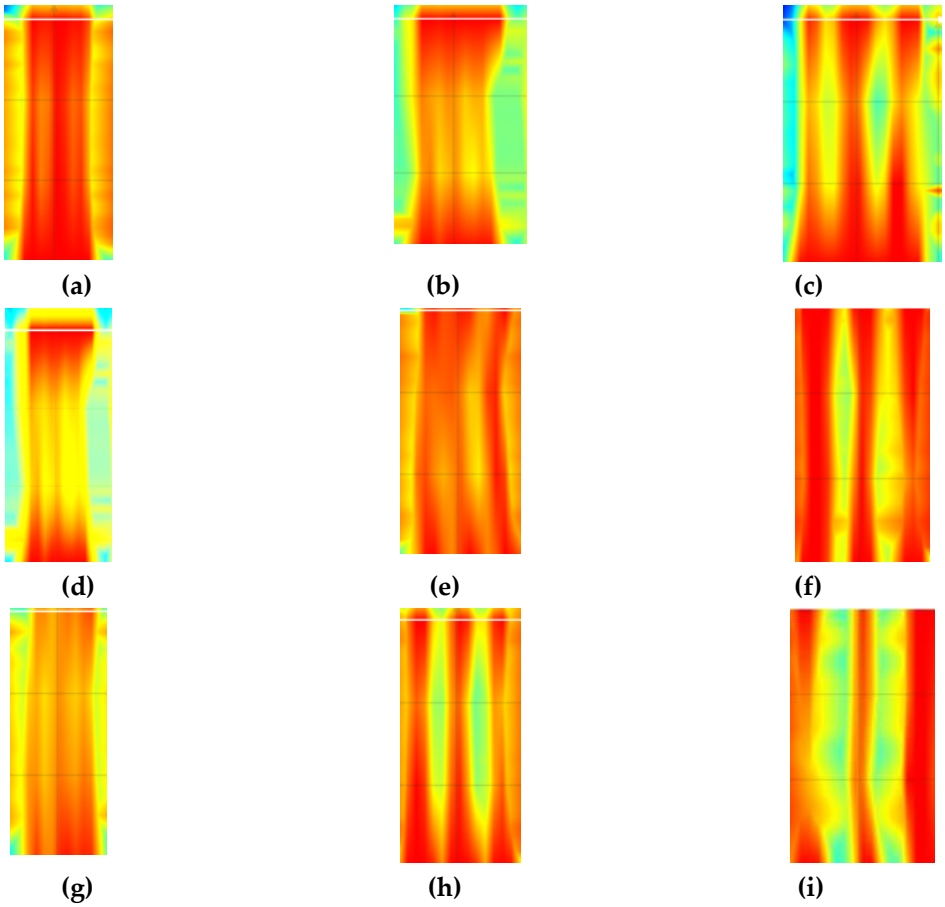

Figure 19. Results from tests performer with the radar equipment (3): (**a**) S-10-20 (result: 3 bars, c_{obs} = 22 mm), (**b**) S-10-30 (3 bars, c_{obs} = 22 mm), (**c**) S-10-40 (3 bars, c_{obs} = 21 mm), (**d**) S-16-20 (3 bars, c_{obs} = 22 mm), (**e**) S-16-30 (3 bars, c_{obs} = 21,= mm), (**f**) S-16-40 (3 bars, c_{obs} = 20 mm), (**g**) S-20-20 (3 bars, c_{obs} = 22 mm), (**h**) S-20-30 (3 bars, c_{obs} = 20 mm), (i) S-20-40 (3 bars, c_{obs} = 20 mm)

7. **Discussion of results**

7.1. AAC precast lintels

7.1.1. Stirrups tests

Direct measurements were taken to analyse the accuracy of conducted tests. Thickness of reinforcement cover in holes made with a 2 mm drill was subjected to direct measurements at tested locations (Fig. 7). Results from these measurement are presented in column 2 of Table 1.

Results from non-destructive testing of 11 inner stirrups of the beam are presented in Table 1 (three last columns of Table) along with estimators of uncertainty according to [33]. The uncertainty of calibration was assumed to be equal to the accuracy of particular devices, and the uncertainty of an experimenter and the random uncertainty were neglected. The real average cover of stirrups was c_{obs} = 28.3 mm, with the standard deviation of 0.87 mm and the variation coefficient of 3%. The estimated average reinforcement cover with the standard uncertainty was 3 ± 0.3 mm (the confidence level 68.3%),and the cover taking into account the maximum uncertainty at the confidence level of 99.7% was equal to 28.3 ± 0.9 mm. The reinforcement nominal cover was c_{nom} = 25 mm, and the execution deviation allowed by the standard EN 13670 [34] was Δ_{minus} = 10 mm. The result obtained from direct measurements was within determined limits. Considering other methods, the obtained average cover was 27 mm, 28.6 mm and 27 mm, while standard and maximum deviations did not exceed ±0.3 mm and ±1.0 mm. Obtained minimum covers measured with every NDT methods were bigger than the determined minimum cover taking into account the dimension deviation. The reinforcement diameter was determined only with the electromagnetic scanner 1. The obtained result

Preprints (www.preprints.org) | NOT PEER-REVIEWED | Posted: 5 March 2019 doi:10.20944/preprints201901.0014.v2

Peer-reviewed version available at Materials 2019, 12, 1168; doi:10.3390/ma12071168

was equal to 6 mm, with the real diameter of 4.5 mm. However, the device manufacturer declares detection of rebars with a diameter from 6 mm.

Diameters of stirrups were calculated on the basis of the obtained radargram and using the equations (5 and 6) and (7). Moving time t_o was determined with the device, and other quantities required for equations were read from the radargram. For equations (5 and 6), the calculated stirrup diameter was 5.6 mm, and in case of the equation (7), the calculated diameter was 5.9 mm. Thus, the determined diameter was greater by 33% and 41% respectively than the real diameter.

Table 1. Measurement results for stirrup reinforcement with each method

Measuring point no.	Cover measured with the method, mm			
	Direct method, c_{obs}	Electromagnetic device (1)	Electromagnetic device (2)	Radar device (3)
1	30.1	27	28.9	27
2	28.1	28	28.6	27
3	28.3	28	29.1	27
4	28.2	28	28.1	27
5	29.1	27	28.6	28
6	27.3	27	28.2	27
7	27.9	27	28.7	27
8	26.9	28	28.3	27
9	28.3	27	28.4	27
10	28.2	27	28.6	27
11	29.0	28	28.7	28
Average cover, c_{obs}:	**28.3**	**27**	**28.6**	**27**
Nominal cover, c_{nom}:	15 mm ≤ c_{nom} ≤ 25 mm			
Calibration uncertainties Δc_{obs}	0.1	1.0	0.1	1.0
Standard deviation, s:	0.87	0.52	0.30	0.40
Standard deviation of the mean value $\bar{s} = \frac{s}{\sqrt{n}}$	0.3	0.2	0.1	0.1
Standard deviation of the calibration $S_d = \frac{\Delta c_{obs}}{\sqrt{3}}$	0.1	0.6	0.1	0.6
Standard uncertainty $S_c = \sqrt{S_d^2 + \bar{s}^2}$	0.3	1	0.1	1
Result with standard uncertainty $c_{mv} \pm S_c$	**28.3±0.3**	**27±1**	**28.6±0.1**	**27±1**
Maximum uncertainty $\Delta c = \Delta c_{obs} + 3\bar{s}$	0.9	1	0.4	1

Preprints (www.preprints.org) | NOT PEER-REVIEWED | Posted: 5 March 2019 doi:10.20944/preprints201901.0014.v2

Peer-reviewed version available at Materials 2019, 12, 1168; doi:10.3390/ma12071168

Table 1. Measurement results for stirrup reinforcement with each method cont.

Measuring point no.	Cover measured with the method, mm			
	Direct method, c_{obs}	Electromagnetic device (1)	Electromagnetic device (2)	Radar device (3)
Result with maximum uncertainty $c_{mv} \pm \Delta c$	**28.3±0.9**	**27±1**	**28.6±0.4**	**27±1**
Minimum cover c_{min}	27.4	26	28.2	26

7.1.2. Tests on longitudinal rebars

Similarly as in case of testing stirrups, rebar cover was directly measured and results are shown in column 2 of table 2. Measurement results are presented in table 2 (three last columns of table) along with estimators of uncertainty according to [33]. The same assumptions were made as for the uncertainty analysis of stirrup location. There were some problems with the comparison of measurement results with the real results because each device detected fewer rebars than the real number. Finally, it was decided to compare test results of the electromagnetic device 1 (Fig. 10a) to real measurements made on extreme rebars in holes drilled in places where electromagnetic measurements were taken (8 measuring points). In case of devices 2 and 3 devices which detected only one rebar, values from holes were compared to value measured for one rebar. Thus, the same values are presented for measuring points 1 and 5, 2 and 6, 3 and 7, 4 and 8 (Fig. 10a) in Table 2. The real average cover of longitudinal rebars was c_{obs} = 29.2 mm, with the standard deviation of 0.7 mm and the variation coefficient of 2.4 mm. The estimated average reinforcement cover with the standard uncertainty was 29.2 ± 0.3 mm (the confidence level 68.3%),and the cover taking into account the maximum uncertainty at the confidence level of 99.7% was equal to 29.2 ± 0.8 mm.

The nominal cover of reinforcement was c_{nom} = 25 mm, and execution deviation allowed by the standard [34] was Δ_{minus} = 10 mm. Thus, the obtained result from direct tests was within determined limits. For other methods, medium-sized covers equal to 34 mm, 27.5 mm and 31 mm were obtained. Standard deviations mostly did not exceed ± 1 mm, and at maximum ± 4 mm. Obtained minimum covers were bigger than minimum values taking into account executive deviations.

In case of main reinforcement testing (beams at the bottom), obtained deviations were considerably greater than in case of stirrup tests (beams on the lateral surface). It should be emphasized that every device used in the tests did not detect the real number of rebars in the main reinforcement. Consequently, the result was burdened with a serious error resulting from the wrong reading of rebars number by research devices.

Table 2. Measurement results for the main reinforcement with method

Measuring point no.	Cover measured with the method, mm			
	Direct method, c_{obs}	Electromagnetic device (1)	Electromagnetic device	Radar device (3)
1	29.1	30	26.2	31
2	28.8	32	27.3	30
3	28.7	35	28.1	31
4	29.2	37	28.4	32
5	29.1	30	26.2	31
6	28.9	32	27.3	30
7	29.2	35	28.1	31
8	30.9	37	28.4	32

Preprints (www.preprints.org) | NOT PEER-REVIEWED | Posted: 5 March 2019 doi:10.20944/preprints201901.0014.v2

Peer-reviewed version available at Materials 2019, 12, 1168; doi:10.3390/ma12071168

Table 2. Measurement results for the main reinforcement with method cont.

Measuring point no.	Cover measured with the method, mm			
	Direct method, c_{obs}	Electromagnetic device (1)	Electromagnetic device	Radar device (3)
Average cover, c_{obs}:	**29.2**	**34**	**27.5**	**31**
Nominal cover, c_{nom}:	15 mm ≤ c_{nom} ≤ 25 mm			
Calibration uncertainties Δc_{obs}	0.1	1.0	0.1	1.0
Standard deviation, s:	0.70	2.9	0.9	0.8
Standard deviation of the mean value, $\bar{s} = \frac{s}{\sqrt{n}}$	0.2	1.0	0.3	0.3
Standard deviation of the calibration $S_d = \frac{\Delta c_{obs}}{\sqrt{3}}$	0.1	0.6	0.1	0.6
Standard uncertainty $S_c = \sqrt{S_d^2 + \bar{s}^2}$	0.3	1	0.3	0.6
Result with standard uncertainty $c_{mv} \pm S_c$	**29.2±0.3**	**34±1**	**27.5±0.3**	**31±0.6**
Maximum uncertainty $\Delta c = \Delta c_{obs} + 3\bar{s}$	0.8	4	1.1	2
Result with maximum uncertainty $c_{mv} \pm \Delta c$	**29.2±0.8**	**34±4**	**27.5±1.1**	**31±2**
Minimum cover c_{min}	28.4	30	26.4	29

7.2. Lightweight concrete specimens

Table 3 presents measurement results for lightweight concrete specimens. There are measured diameters $ø_{obs}$, number of rebars n_{obs} and size of c_{obs}. A shaded field shows measured values which were the same as nominal values in models. The analysis of values in the table indicates that the number of rebars having a diameter greater than 10 mm could be identified at spacing greater than 20 mm using the electromagnetic equipment (1) and (2). Measured values closest to nominal values of diameters were observed at rebar spacing of 30 mm. The equipment showed similar diameters, but the false number of rebars at smaller spacing. The average ratio $ø_{obs}$ / $ø_{nom}$ in accordance with electromagnetic methods (1) and (2) was 1.1. If the accuracy of indications of the electromagnetic equipment of the order of ca. ±1,0 mm was taken into account during the analysis of measurements, then results from measuring diameters with these methods could be considered as reliable at spacing larger than 20 mm and for diameters greater than 10 mm. Rebar diameters could not be read in case of using the radar equipment (3). Therefore, diameters were calculated in a similar way to precast lintel beam, using equations (5 and 6) and (7). More satisfactory compliance with nominal values was achieved using equations (5 and 6). And those values are shown in Table 3. Measured diameters were greater by ca. 15% than nominal values.

Rebar covers could be measured using all those methods. Electromagnetic methods (1) and (2) provided the average cover of 21.6 mm and 17.3 mm, respectively. And difference from the nominal value was ±5,0 mm, that is, within limits of allowable execution deviations Δ_{minus} = 10 mm specified by the standard [34]. The radar method ensured more precise results as the measured average cover was 21.1 mm, and the maximum difference from the nominal value was +2.0 mm.

Table 3. Test results for lightweight concrete specimens

Geometry of models				Results from tests conducted with the equipment (1), (2) or (3)								
Reinforcement diameter ø, mm	Number of rebars n_{nom}	Rebar spacing a_{nom}, mm	Reinforcement cover c_{nom}, mm	$ø_{obs}$, mm			n_{obs}, mm			c_{obs}, mm		
				(1)	(2)	(3)*	(1)	(2)	(3)	(1)	(2)	(3)
10	3	20	20	8	8	11.9	2	1	3	25	20	22
		30		8	10	11.8	3	3	3	20	19.3	22
		40		10	9	11.5	3	3	3	21	19.3	21
16	3	20	20	30	17	18.8	2	3	3	25	15.5	22
		30		16	15	18.2	3	3	3	18	16.4	21
		40		20	14	17.8	3	3	3	20	16.5	20
20	3	20	20	20	19	23.3	3	3	3	25	15	22
		30		20	19	23.1	3	3	3	18	15.4	20
		40		20	18	22.8	3	3	3	22	18.3	20

(1) – electromagnetic device (fig 12a), (2) – electromagnetic device (fig 12b), (3) – radar device (fig.12c), * * values obtained from equations (5 and 6)

Tests conducted on lightweight concrete specimens confirmed results from tests on precast lintel beam. The greatest inaccuracies of measurements were observed for rebars with lower diameters (≤10 mm), at small spacing (≤20 mm). For greater diameters (≥16 mm), even small spacing did not affect detection of the reinforcement, including the number of rebars, their diameter, and the thickness of concrete cover. The radar equipment provided more precise size of concrete cover compared to the electrical equipment. Rebar diameters calculated from the radargram were overcalculated by ca. 15 in comparison to nominal values. However, considerably better results in measuring diameters were noticed in case of electromagnetic diameters.

Tests indicated that a measurement error was significant particularly for measuring structures reinforced with small diameter bars at a small spacing. This could lead to improper interpretation of test results, and consequently to wrong calculation analyses for structures.

8. Conclusions

Conducted tests demonstrated the occurrence of some limitations of two popular methods for detecting reinforcement location in the structure. Devices were able to correctly detect rebars, even these of small diameters, providing that they were located at an adequate spacing. Devices for scanning reinforcement had some problems with defining the correct quantity and diameter of rebars placed close to each other, at a distance shorter than 2÷3 diameters.

Results obtained for covers measured with electromagnetic and radar devices did not significantly differ in terms of an average value. For the real cover, differences did not exceed acceptable level of few percent (<5%). There was no clear tendency to state that any of methods artificially distorted indications, for instance, due to the simplification for measurement method validation. However, it should be emphasized that minimal covers determined by all non-destructive techniques were bigger than the minimal cover specified with regard to size deviations (accepted by standard EN 13670:2011 [34]) and obtained by direct measurements. Thus, tests on existing building can generate an error which is greater than the acceptable execution deviation. This can lead to wrong conclusions about the accuracy of a building. Measurements taken in the existing structure should be analysed with caution because the incorrect interpretation of measurement results for reinforcement

location in the cross-section can cause a reduction in safety coefficient for steel $\gamma_{S,red1}$ from 1.15 to 1.1 (acc. to EC-2 [35]) and unintentional reduction of safety level in particularly significant support zones of reinforced concrete structures and prestressed structures.

Studies aiming at connecting both methods, consisting in connecting scans taken with devices operating according to the electromagnetic and radar method, seem to be reasonable. Hybrid devices are likely to generate accurate results, especially in terms of measuring reinforcement diameters.

Author Contributions: Conceptualization, Ł.D. and R.J.; methodology, Ł.D. R.J and W.M.; formal analysis, Ł.D. and R.J and W.M.; investigation, Ł.D, W.M and R.J.; writing—original draft preparation, Ł.D.; writing—review and editing, Ł.D. and R.J.; visualization, W.M. and Ł.D.; supervision, R.J and Ł.D.

Acknowledgements: The authors would like to express particular thanks to Solbet Sp. z o.o. company, for supply of materials used during the research works. We would also like to thank Hilti, Proceq and Viateco for providing research equipment.

Conflicts of Interest: The authors declare no conflicts of interest.

References

1. Malhorta V.M., Carino N.J., *Handbook on nondestructive testing of concrete*, Second edition. CRC Press LCC, ASTM International, Boca Raton, London, New York, Washington D.C. 2004.
2. Bungey J.H., Millard S.G., Grantham M.G., *Testing of concrete in structures*, 4th edition, Taylor & Francis, London and New York 2006.
3. Drobiec Ł., Jasiński R., Piekarczyk A. *Diagnostic testing of reinforced concrete structures*. Methodology, field tests, laboratory tests of concrete and steel. Wydawnictwo Naukowe PWN, Warszawa 2013. (in-Polish).
4. Hoła, J.; Schabowicz, K. State-of-the-art non-destructive methods for diagnostic testing of building structures–anticipated development trends. Archives of Civil and Mech. Engineering **2010**, 10, pp. 5-18.
5. Drobiec Ł., Diagnosis of industrial structures. Materiały Budowlane No 2015/2, pp. 32÷-34.
6. Zima B., Rucka M., Detection of debonding in steel bars embedded in concrete using guided wave propagation. Diagnostyka, **2016**, 3, pp. 27-34.
7. Hoła J., Bień J., Schabowicz K., Non-destructive and semi-destructive diagnostics of concrete structures in assessment of their durability. Bulletin of the Polish Academy of Sciences, **2015**, 63, pp. 87-96.
8. Ma X., Liu H., Wang M.L., Birken R., Automatic detection of steel rebar in bridge decks from ground penetrating radar data. Journal of Applied Geophysics, **2018**, 158, pp. 93-1
9. ISO/IEC, Guide 99:2007 *International vocabulary of metrology – basic and general concepts and associated terms*.
10. Chady, T.; Frankowski, P.K. Electromagnetic evaluation of reinforced concrete structure. Review of Progress in Quantitative Nondestructive Evaluation: Volume 32. 15–20 July 2012, Denver, Colorado, USA. AIP Conference Proceedings 2013, 1511. p.1355-1362
11. Drobiec, Ł.; Górski, M.; Krzywoń, R.; Kowalczyk, R. Comparison of non-destructive electromagnetic methods of reinforcement detection in RC structures. Challenges for Civil Construction CCC 2008, Porto, Portugal, 16-18 April 2008.
12. Szymanik, B.; Frankowski, P.K.; Chady, T.; Robinson, C.; Chelliah, A.J. Detection and Inspection of Steel Bars in Reinforced Concrete Structures Using Active Infrared Thermography with Microwave Excitation and Eddy Current Sensors. Sensors **2016**, 16.
13. Frankowski, P.K.; Sikora, R.; Chady, T. Identification of rebars in a reinforced mesh using eddy current method. 42nd Annual Review of Progress in Quantitative Nondestructive Evaluation: Incorporating the 6th European-American Workshop on Reliability of NDE. 26–31 July 2015, Minneapolis, Minnesota, USA. AIP Conference Proceedings 2016, 1706.
14. Hola, J.; Schabowicz, K. Application of artificial neural networks to determine concrete compressive strength based on non-destructive tests. Journal of Civil Engineering and Management **2005**, 11, pp. 23-32.
15. Sivasubramanian, K.; Jaya, K.P.; Neelemegam, M.; Covermeter for identifying cover depth and rebar diameter in high strength concrete. Internat. Journal of Civil and Struct. Engineering **2013**, 3, pp. 557-563.
16. Lachowicz, J.; Rucka, M. Application of GPR method in diagnostics of reinforced concrete structures. Diagnostyka **2015**, 16.
17. Lachowicz, J.; Rucka, M. 3-D finite-difference time-domain modelling of ground penetrating radar for identification of rebars in complex reinforced concrete structures. Archives of Civil and Mechanical Engineering **2018**, 18, pp. 1228 – 1240.

18. Agred, K; Klysz, G.; Balayssac, J.P. Location of reinforcement and moisture assessment in reinforced concrete with a double receiver GPR antenna. Constr. and Building Materials **2018**, 188, pp. 1119–1127.
19. Shaw, M.R.; Millard, S.G.; Molyneaux, T.C.K.; Taylor, M.J.; Bungey, J.H. Location of steel reinforcement in concrete using ground penetrating radar and neural networks. NDT&E International **2005**, 38, pp. 203-212
20. Chang, C.W.; Lin C.H.; Lien, H.S. Measurement radius of reinforcing steel bar in concrete using digital image GPR. Construction and Building Materials **2009**, 23, pp. 1057-1063.
21. Shihab S., Al-Nuaimy W., Radius estimation for cylindrical objects detected by ground penetrating radar. Subsurface Sensing Technologies and Applications **2005**, 6, pp. 151-166.
22. Ristic, A.V.; Petrocacki, D.; Govedarica, M.; A New Method to Simultaneously Estimate the Radius of A Cylindrical Object and the Wave Propagation Velocity From GPR Data. Computers and Geosciences **2009**, 35, pp.1620 1630.
23. Idi B.Y., Kamarudin M.N.: Utility Mapping with Ground Penetrating Radar: an Innovative Approach. Journal of American Science **2011**, 7, pp. 644 649.
24. Zanzi, L.; Arosio, D. Sensitivity and accuracy in rebar diameter measurements from dual-polarized GPR data. Construction and Building Materials **2013**, 48, pp. 1293-1301.
25. Mechbal, Z.; Khamlichi, A. Determination of concrete rebars characteristics by enhanced postprocessing of GPR scan raw data. NDT&E International **2017**, 89, pp. 30-39.
26. Wei, J.S.; Hashim, M.; Marghany, M. New approach for extraction of subsurface cylindrical pipe diameter and material type from ground penetrating radar image. 31st , ACRS 2010, vol. 2, 2010, s. 1187-1193.
27. Alhsanat, M.B.; Wan Hussin, W.M.A. A New Algorithm to Estimate the Size of an Underground Utility via Specific Antenna, PIERS Proceedings, Marrakesh, Maroko, 20-23 marca 2011, s. 1868-1870.
28. Wiwatrojanagul, P.; Sahamitmongkol, R.; Tangtermsirikul, S.; Khamsemanan, N. A new method to determine locations of rebars and estimate cover thickness of RC structures using GPR data. Construction and Building Materials **2017**, 140, pp. 257-273.
29. Wiwatrojanagul, P.; Sahamitmongkol, R.; Tangtermsirikul, S. A method to detect lap splice in reinforced concrete using a combination of covermeter and GPR. Constr. and Build. Materials **2018**, 173, pp. 481-494.
30. Drobiec, Ł.; Jasiński, R.; Mazur, W. Precast lintels made of autoclaved aerated concrete – test and theoretical analyses. Cement Wapno Beton **2017**, 5, pp. 339-413.
31. Mazur, W.; Drobiec, Ł.; Jasiński, R. Research of Light Concrete Precast Lintels. Procedia Engineering **2016**, 161, pp. 611-617.
32. Mazur, W.; Drobiec, Ł.; Jasiński, R. Research and numerical investigation of masonry - AAC precast lintels interaction. Procedia Engineering **2017**, 193, pp. 385 – 392.
33. JCGM 100:2008 *Evaluation of measurement data. Guide to the expression of uncertainty in measurement*.
34. EN 13670:2011 *Execution of concrete structures*.
35. EN 1992-1-1 *Eurocode 2: Design of concrete structures - Part 1-1: General rules and rules for buildings.*